JOURNAL OF MECHANICAL ENGINEERING AND SCIENCES (JMES)
ISSN: 2289-4659 e-ISSN: 2231-8380
VOL. 15, ISSUE 1, 7918 – 7935
DOI: https://doi.org/10.15282/jmes.15.1.2021.25.0625

ORIGINAL ARTICLE

The onset of magnetic nanofluid convection because of selective absorption of radiation

Amit Mahajan[1] and Mahesh Kumar Sharma[2]*

[1] Department of Applied Sciences,National Institute of Technology Delhi, Narela, Delhi, 110040, India
[2] Department of Mathematics, Maharaja Agrasen University, Baddi, Himachal Pradesh, 174103, India

ABSTRACT – This article reports a linear stability analysis of the onset of convection stimulated by selective absorption of radiation in a horizontal layer of magnetic nanofluid (MNF) under the impact of an external magnetic field. The Chebyshev pseudospectral method is utilized to obtain the numerical solution for water-based magnetic nanofluids (MNFs). The confining boundaries of the magnetic nanofluid layer are considered to be rigid–rigid, rigid–free, and free–free. The results are derived for two different conditions, viz., when the system is heated from the below and when the system is heated from the above. It is observed that an increase in the value of the Langevin parameter α_L, diffusivity ratio η and a decrease in the value of nanofluid Lewis number Le, the parameter Y which represents the impact of selective absorption of radiation and modified diffusivity ratio N_A delays the onset of MNF convection for both the two configurations. Moreover, as the value of concentration Rayleigh number R_n increases, the convection commences easily when the system is heated from the below, whereas the onset of MNF convection gets delayed as the system is heated from the above.

ARTICLE HISTORY
Received: 01st Apr 2020
Revised: 12th Sept 2020
Accepted: 14th Sept 2020

KEYWORDS
Magnetic nanofluids; radiation absorption; penetrative convection; magnetic field; Heat source

INTRODUCTION

A primary study of convection stimulated by selective absorption of radiation in a stably stratified fluid layer was conducted experimentally by Krishnamurti [1]. The author considers a stably stratified fluid layer of water, which was assumed to be heated from below or above under the presence of a pH indicator called thymol blue. She performed both linear instability analysis and weakly nonlinear stability analysis in order to observe the form of convection patterns. The convection mechanism reported in her study was a penetrative one which generates due to the presence of an internal heat source through the absorption of radiation. The mechanism of penetrative convectionoccurs due to the penetration of buoyancy-driven motion into stably stratified layers [2]. Straughan [3] conducted a detailed investigation of the convection model developed by Krishnamurti [1]. He considered the bounding surfaces being fixed and analyzed the convective instability by applying linear and nonlinear stability analysis. The author reported that his results endorse the Krishnamurti's work, and the model suggested by Krishnamurti is very impressive.Using Krishnamurti's model, Hill [4] performed a linear and nonlinear instability analysis to investigate the onset of convective instability stimulated by selective absorption of radiation in a fluid-saturated porous layer. Later, following Krishnamurti's work, Chang [5] studied the convective instability in a two-layer system by employing the linear stability theory. The author used the Chebyshev method and derived the results for the two cases, viz., when the system is heated from below and when the system is heated from above. For more interesting related studies, the reader may refer to [2, 6, 7].

Nanofluids are the solid-liquid composite materials in which a large number of solid nanofibers or nanoparticles of the dimension of the order 1-100 nm are dispersed in a base liquid. A comprehensive study of convective transport in nanofluid was conducted by Buongiorno [8]. He developed a new model which incorporates the effects of two significant mechanisms, viz., Brownian diffusion, and thermophoresis. A foremost study of convective instability in a nanofluid layer was conducted by Tzou [9]. The author used the model suggested by Buongiorno and reported that nanofluids are less stable as compared to regular fluids. Later, the same problem was re-investigated by Nield and Kuznetsov [10], where the authors consider different types of parameters (non-dimensional).They reported that oscillatory instability may exist for a bottom-heavy nanoparticle distribution. Later, the authors re-examined this problem for more realistic boundary conditions and reported that the non-stationary convection can no longer occur with the change in boundary conditions [11]. Since then, many interesting studies have been conducted in the area of nanofluid convection [12-24]. Recently, Mahian et al. [25] conducted a comprehensive review of the latest development in the modeling of nanofluid flows and heat transfer.In another part of the review [26], the authors discussed the important computational methods (such as the finite difference method, finite element method, finite volume method, etc.) for solving the equations related to nanofluid flow.The effect of the magnetic field at the onset of convective instability in a nanofluid layer has its importance in several physical phenomena concerned with astrophysics and geophysics, biochemical engineering, and chemical engineering

*CORRESPONDING AUTHOR | M. K. Sharma | ✉ mksharma.maths@gmail.com

[27]. Gupta et al. [27] examined the thermal instability in a layer of nanofluid under the appearance of an external magnetic field by applying the linear stability analysis. Yadav et al. [28]studied the effect of an external magnetic field on the onset of natural convection in a nanofluid layer which was assumed to be electrically conducting.Recently, Yadav [29]studied the combined effect of both magnetic field and pulsating throughflow on convective instability in a nanofluid, and analyzed the impact of various significant parameters.Kolsi et al. [30] investigated the effect of an applied magnetic field on the production of entropy in the case of the natural convection of a low Prandtl liquid metal in a cubic cavity.Maatki et al. [31] examined the double diffusion convection in a cubic cavity teemed with the binary mixture subject to a magnetic field.Another interesting phenomena, known as mixed convection have its significance in various industrial applications like coating or continuous reheating furnaces, solidification of ingots, and float glass manufacturing [32]. A numerical investigation of the impact of an external magnetic field at the onset of nanofluid mixed convection heat transfer was conducted by Rashidi et al. [33]. Over the past few years, the impact of an external magnetic field at the onset of nanofluid convection and nanofluid mixed convection has been studied by several researchers under various aspects[34-36].

Magnetic nanofluids, i.e. nanofluids consisting of magnetic nanoparticles like cobalt, iron, nickel, and their oxides suspended in a non-magnetic carrier liquid, have both fluids as well as magnetic properties [37]. A foremost investigation of convective instability for a layer of ferromagnetic fluid under the existence of an applied external magnetic field was organized by Finlayson [38]. He introduced a new mode of thermo-mechanical interaction and analyzed the convective instability problem in two different cases, viz., in the presence of vertical body force and in the absence of vertical body force. Following Finlayson's work, several kinds of research in the area ferrofluid convection have been performed in recent years. Mahajan et al. [39] performed a linear instability analysis to examine the convective stability in a magnetic nanofluid (MNF) layer under the existence of an external magnetic field. The impact of the three significant mechanisms, namely, (i) Brownian motion, (ii) thermophoresis, and (iii) magnetophoresis were considered in their study. Mahajan and Sharma [40] further investigated the onset of convective instability in a MNF-saturated porous medium layer by employing the linear stability theory.Sheikholeslami et al. [41] employed CVFEM (known as Control Volume-based Finite Element Method) to study the impact of magnetic field dependent viscosity on MHD nanofluid heat transfer.Sheikholeslami [42] examined the free convection of a MNF in a porous curved cavity under the influence of a magnetic source (external). The reader may refer to [43-47] for more related studies in the literature.

The present work extends the study of Mahajan and Sharma [48], where the authors investigated the convective instability because of the selective absorption of radiation in a magnetic nanofluid saturated porous medium.The authors assumed that the fluid flow follows Darcy's law with permeability K. However, no such an assumption for the fluid flow is considered in the present work. The main objective of this work is therefore to examine the onset of convection stimulated because of the selective absorption of radiation in a horizontal layer of MNF subject to the influence of an external applied magnetic field. Due to the existence of thymol blue, a motion, known as penetrative convection occurs in the MNF layer because of the internal heating through the incorporation of radiation. The internal heat source generates a temperature gradient (non-uniform) which in turn regulates the onset of convection. This type of variation in temperature gradient gives rise to a variation in nanoparticles and magnetic field. These variations have significant importance in controlling the convection in various practical applications (e.g., continuous operation refrigerators). To understand the requirements of these applications, the study of penetrative convection in a MNF layer is compulsory. In the present work, we solved the eigenvalue problem for Rigid-Rigid (R-R), Rigid-Free (R-F), and Free-Free (F-F) boundary conditions for water based MNF by selecting the Chebyshev pseudospectral method. The preparation of water based MNFs is of renewed interest nowadays because of its importance in biomedical applications. In the present study, physical properties of water based MNF are considered as: density $\rho_f = 1180,$ thermal conductivity $k_1 = 0.59,$ magnetic saturation $M_s = 15,900,$ viscosity $\mu = 0.007,$ thermal expansion coefficient $\alpha = 5.2e-4,$ Prandtl number $\mathrm{Pr} = 42.1.$ These values are taken from the book by Rosensweig [49] and the article by Kaloni and Lou [50]. The effects of Langevin number α_L, the concentration Rayleigh number R_n, diffusivity ratio $\eta,$ nanofluid Lewis number Le , the parameter Y (ratio of internal heating to boundary heating) and the modified diffusivity ratio N_A are studied at the onset of MNF convection. Outcomes results are illustrated graphically and in tabular form for two different conditions, viz., when the system is heated from the below and when the system is heated from the above.

FORMULATION OF THE PROBLEM

The schematic of considered system is presented in Figure 1. Here, we consider a horizontal layer of incompressible MNF under the presence of a magnetic field (vertical) $\mathbf{H} = H_0^{ext}\mathbf{k}$.

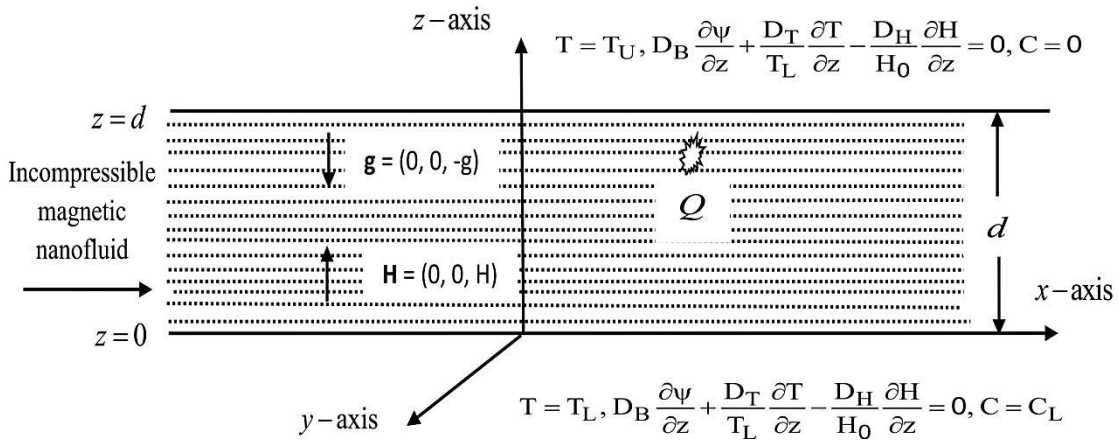

Figure. 1. Schematic diagram of the system

The MNF is assumed to be enclosed between two planes, viz., $z = 0$ and $z = 0$. The term T_L represents the temperature at the lower boundary, whereas T_U stands for the temperature at the upper boundary. The nanoparticle flux is assumed to be zero on the boundaries. The system also contains an internal heat source with strength Q which depends upon the quantity of radiation absorbed.

The governing equations under the assumption of Boussinesq approximation are as follows[1, 11, 38, 45, 51].The continuity equation:

$$\nabla \cdot \mathbf{v} = 0 \tag{1}$$

The momentum equation:

$$\rho_f \left(\frac{\partial \mathbf{v}}{\partial t} + \mathbf{v} \cdot \nabla \mathbf{v} \right) = -\nabla p + \mu \nabla^2 \mathbf{v} + \mu_0 M \nabla H - \rho g \mathbf{k} \tag{2}$$

The equation of nanoparticle:

$$\frac{\partial \psi}{\partial t} + \mathbf{v} \cdot \nabla \psi = \nabla \cdot \left(D_B \nabla \psi + D_T \frac{\nabla T}{T_L} - D_H \frac{\nabla H}{H_0} \right) \tag{3}$$

The equation of temperature:

$$(\rho c)_f \left(\frac{\partial T}{\partial t} + \mathbf{v} \cdot \nabla T \right) = \nabla \cdot (k_1 \nabla T) + \rho_p c_p \left(D_B \nabla T \cdot \nabla \psi + D_T \frac{\nabla T \cdot \nabla T}{T_L} - D_H \frac{\nabla T \cdot \nabla H}{H_0} \right) + Q \tag{4}$$

The thymol blue concentration equation:

$$\frac{\partial C}{\partial t} + \mathbf{v} \cdot \nabla C = k_c \nabla^2 C \tag{5}$$

In Eq. (2), the terms $\mathbf{v}$, ρ_f, p, μ, t, μ_0, g, M and $\mathbf{k}$ represent the velocity vector, fluid density, pressure term, fluid viscosity, time, vacuum magnetic permeability, gravity, magnetization and vertically upward unit vector respectively. Moreover, the parameter ρ is the overall density defined as $\rho = \psi \rho_p + (1-\psi)\rho_f (1 - \alpha (T - T_L))$. Here, it is assumed that the density in the buoyancy force is independent from (the thymol blue concentration) [3].

In addition, the terms $D_B, \psi, D_T, T_L, D_H, (\rho c)_f, k_1, \rho_p, c_p$ and C appearing in the Eqs. (3) to (5) stand for Brownian diffusion coefficient, magnetic nanoparticle volume fraction, thermophoretic diffusion coefficient, temperature at the lower boundary, magnetophoretic coefficient, MNF volumetric heat capacity, MNF thermal conductivity, magnetic nanoparticle density, nanoparticle specific heat, thymol blue diffusivity, and concentration respectively. Following the work of Krishnamurti [1], a relationship (linear) $Q = (\rho c)_f \alpha' C$, is assumed between C and Q, where α' is a proportionality constant.

To investigate the MNF convection under the impact of an external magnetic field, the Maxwell equations must be solved simultaneously with the Eqs. (1) to (5). In the magnetostatic limit, the Maxwell equations take the following form:

$$\nabla \cdot \mathbf{B} = 0, \nabla \times \mathbf{H} = 0, \tag{6}$$

where $\mathbf{B}$ stands for the magnetic induction.

Moreover, **B** is related with **M** and **H** as:

$$\mathbf{B} = \mu_0(\mathbf{M}+\mathbf{H}). \tag{7}$$

Thereafter, we linearized the magnetic equation of state about H_0, T_L and ψ_0 as suggested by Finlayson [38],

$$\mathbf{M} = \frac{\mathbf{H}}{H}[M_0 + \chi(H-H_0) - K_m(T-T_h) + K_p(\psi-\psi_0)], \tag{8}$$

where M_0 represents the constant mean value of magnetization and $K_m = \chi H_0 / T_0, K_p = \chi H_0 / \psi_0$ are the magnetic coefficients.

For a specific value of the parameter α_L, the two parameters χ and χ_2 (chord magnetic susceptibility) is evaluated as [49]:

$$\alpha_L = \frac{mH_0}{k_B T_0} = \begin{cases} \square\ 1,\ \chi = \dfrac{M_s m}{3k_B T_0},\ \chi_2 = \chi, \\ \square\ 1,\ \chi = \dfrac{M_s m}{k_B T_0} L(\alpha_L),\ \chi_2 = \dfrac{M_s}{T_0} L(\alpha_L), \\ \square\ 1,\ \chi = \dfrac{M_s k_B T_0}{m H_0^2},\ \chi_2 = \dfrac{M_s}{H_0}\left(1-\dfrac{1}{\alpha_L}\right). \end{cases}$$

The boundary conditions are considered as [11, 52]:

$$\left.\begin{aligned} w = 0, T = T_L, D_B \frac{\partial \psi}{\partial z} + \frac{D_T}{T_L}\frac{\partial T}{\partial z} - \frac{D_H}{H_0}\frac{\partial H}{\partial z} = 0, C = C_L \quad \text{at} \quad z = 0, \\ w = 0, T = T_U, D_B \frac{\partial \psi}{\partial z} + \frac{D_T}{T_L}\frac{\partial T}{\partial z} - \frac{D_H}{H_0}\frac{\partial H}{\partial z} = 0, C = 0 \quad \text{at} \quad z = d, \end{aligned}\right\} \tag{9}$$

with $\frac{\partial w}{\partial z} = 0$ and $\frac{\partial^2 w}{\partial z^2} = 0$ on a rigid surface and stress-free surface respectively.

In the above set of boundary conditions, it is considered that the temperature remains fixed at both the boundaries. Whereas, the magnetic nanoparticle flux which consist the impact of three significant mechanisms, namely Brownian motion, thermophoresis, and magnetophoresis is considered to be zero on the boundaries. This is so because, as reported by the researchers Nield and Kuznetsov [11], the considered boundaries are more realistic physically.

The governing Eqs. (1) to (8) are made dimensionless as:

$$(u^*, v^*, w^*) = (u, v, w)d/\kappa, \psi^* = \frac{\psi}{\psi_0}, (x^*, y^*, z^*) = (x, y, z)/d, t^* = (\kappa/d^2)t,$$

$$p^* = (d^2/\mu\kappa)p, T^* = \left(\sqrt{\frac{\rho_f g\alpha d^3}{\mu\kappa |T_L - T_U|}}\right)T, H^* = H/H_0, M^* = M/M_0.$$

Here $\kappa = \dfrac{k_c}{(\rho c)_f}$ is the thermal diffusivity. Note that $K|T_L - T_U| = (T_L - T_U)$, where $K = \text{sign}\left(T_L - T_U\right)$. The value of K depends on whether the layer is heated from below or above. For a layer which is heated from below, K takes the value +1 and K becomes -1 when the layer is heated from above.

Thus, after abandon the asterisks *, we derive the following dimensionless form of Eqs. (1) to (8):

$$\nabla\cdot\mathbf{v} = 0, \tag{10}$$

$$\frac{1}{Pr}\left(\frac{\partial \mathbf{v}}{\partial t} + \mathbf{v}\cdot\nabla\mathbf{v}\right) = -\nabla p + \nabla^2\mathbf{v} + \lambda_1 M\nabla H - \left(R_n\psi - RT + Ra_N T\psi - \rho_1\psi + \rho_2\right)\mathbf{k}, \tag{11}$$

$$\frac{\partial \psi}{\partial t}+\mathbf{v}\cdot\nabla\psi=\frac{1}{Le}\nabla^2\psi+\frac{N_A}{Le}\nabla^2 T-\frac{N'_A}{Le}\nabla^2 H, \tag{12}$$

$$\frac{\partial T}{\partial t}+\mathbf{v}\cdot\nabla T=\nabla^2 T+\frac{N_B}{Le}(\nabla\psi\cdot\nabla T)+\frac{N_A N_B}{Le}(\nabla T\cdot\nabla T)-\frac{N'_A N_B}{Le}(\nabla H\cdot\nabla T)+YRC, \tag{13}$$

$$\frac{\partial C}{\partial t}+\mathbf{v}\cdot\nabla C=\eta\nabla^2 C, \tag{14}$$

$$\mathbf{M}=\frac{\mathbf{H}}{H}\left\{\frac{\chi}{1+\chi}H-\frac{M_1}{M_2}T+\frac{M'_1}{M'_2}\phi+\frac{\chi_2-\chi}{1+\chi}\right\}\times\frac{(1+\chi)}{\chi_2}, \tag{15}$$

$$\chi_2\nabla\cdot\mathbf{M}+\nabla\cdot\mathbf{H}=0. \tag{16}$$

In Eqs. (11) to (16),

$$R_n=\frac{(\rho_p-\rho_f)\psi_0 g d^3}{\mu\kappa},\ Pr=\frac{\mu}{\rho_f\kappa},\ Le=\frac{\kappa}{D_B},\ R=\sqrt{\frac{\rho_f g\alpha d^3|T_L-T_U|}{\mu\kappa}},\ N'_A=\frac{D_H}{D_B\psi_0},$$
$$N_A=\frac{D_T}{D_B T_L\psi_0}\sqrt{\frac{\mu\kappa|T_L-T_U|}{\rho_f g\alpha d^3}},\ N_B=\frac{(\rho c)_p}{(\rho c)_f}\psi_0,\ Y=\frac{\alpha' C_L d^2}{\kappa|T_L-T_U|},\ \eta=\frac{k_c}{\kappa},\ M_2=\frac{\mu_0\chi H_0^2}{\rho_f g\alpha d T_h},$$
$$M'_2=\frac{\mu_0\chi H_0^2}{\rho_f g\alpha d\psi_0},\ M_1=\frac{\mu_0\chi^2 H_0^2}{\rho_f g\alpha d(1+\chi)T_L^2}\sqrt{\frac{\mu\kappa|T_L-T_U|}{\rho_f g\alpha d^3}},\ M'_1=\frac{\mu_0\chi^2 H_0^2}{\rho_f g\alpha d(1+\chi)\psi_0}$$

are the concentration Rayleigh number, Prandtl number, nanofluid Lewis number, square root of thermal Rayleigh number, modified diffusivity ratios $\left(N'_A,\ N_A\right)$, modified particle-density increment, ratio of internal heating to boundary heating, diffusivity ratio, magnetic parameters $\left(M_2,\ M'_2, M_1,\ M'_1\right)$ respectively. Moreover, the parameters $\rho_1=(\rho_f g\psi_0\alpha d^3 T_L)/(\mu\kappa)$, $\rho_2=(\rho_f(1+\alpha T_L)gd^3)/(\mu\kappa)$, $Ra_N=\psi_0 R$ and $\lambda_1=(\mu_0 M_0 H_0 d^2)/(\mu\kappa)$ represent some non-dimensional group. We would like to mention here that the thermal Rayleigh number for the present problem is defined as $Ra=R^2$.

The boundary conditions (9) become (in non-dimensional form):

$$\left.\begin{aligned} w=0, T=T_L\sqrt{\frac{\rho_f g\alpha d^3}{\mu\kappa|T_L-T_U|}}, \frac{\partial\psi}{\partial z}+N_A\frac{\partial T}{\partial z}-N'_A\frac{\partial H}{\partial z}=0, C=1, \quad \text{at} \quad z=0,\\ w=0, T=T_U\sqrt{\frac{\rho_f g\alpha d^3}{\mu\kappa|T_L-T_U|}}, \frac{\partial\psi}{\partial z}+N_A\frac{\partial T}{\partial z}-N'_A\frac{\partial H}{\partial z}=0, C=0, \quad \text{at} \quad z=1, \end{aligned}\right\} \tag{17}$$

together with $\frac{\partial w}{\partial z}=0$ and $\frac{\partial^2 w}{\partial z^2}=0$ on a rigid surface and stress-free surface respectively

BASIC SOLUTION

The solution for the basic state has the following form:

$$p=p_b(z),\ \mathbf{v}=0,\ T=T_b(z),\ \psi=\psi_b(z),\ C=C_b(z),\ M=M_b(z),\ H=H_b(z). \tag{18}$$

Using (18), Eqs. (11) to (16) are simplified as follows:

$$-\frac{dp_b}{dz}+\lambda_1 M_b\frac{dH_b}{dz}-R_n\psi_b+RT_b-Ra_N T_b\psi_b+\rho_1\psi_b-\rho_2=0, \tag{19}$$

$$\frac{d^2\psi_b}{dz^2} + N_A \frac{d^2T_b}{dz^2} - N'_A \frac{d^2H_b}{dz^2} = 0, \tag{20}$$

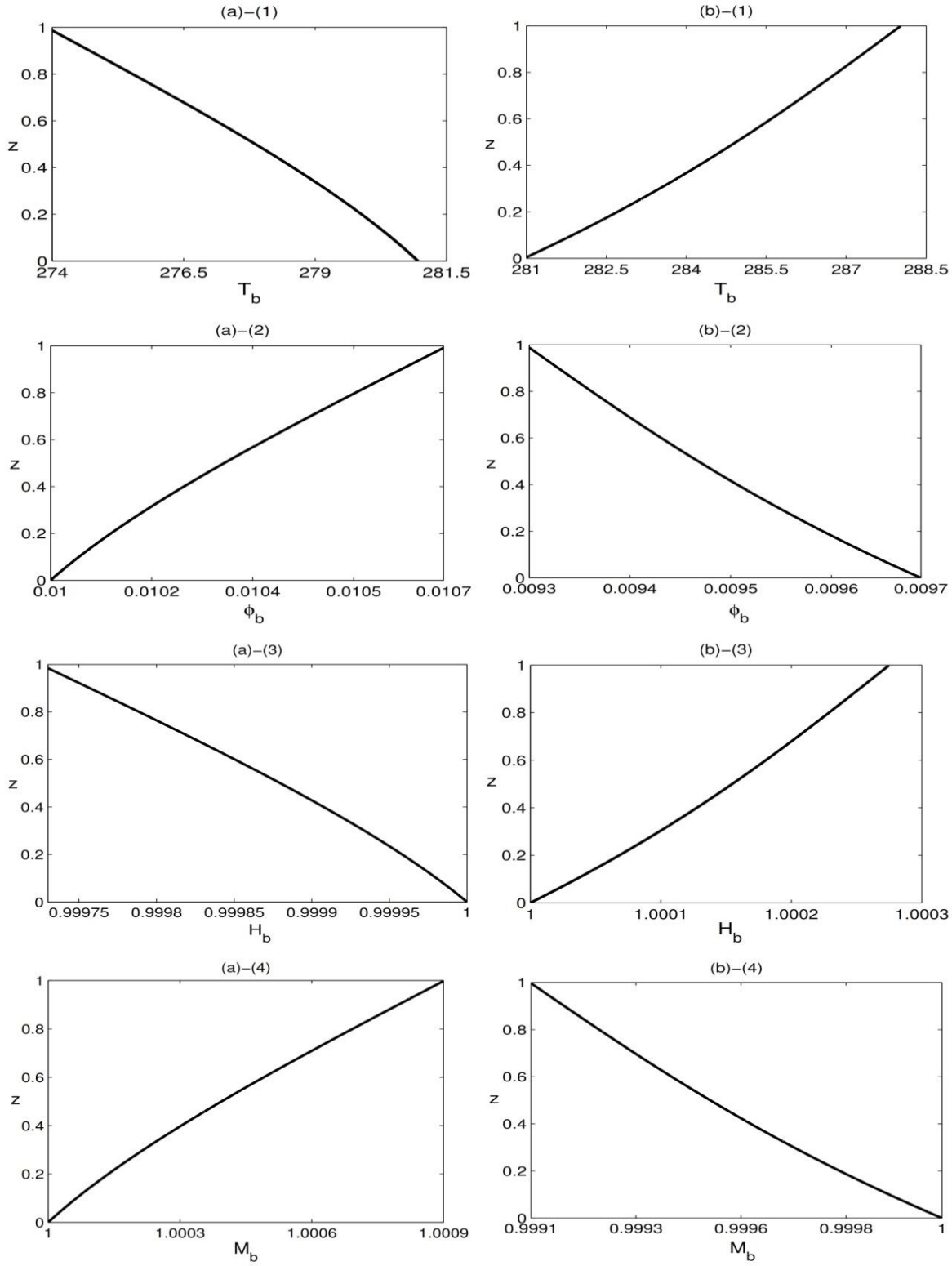

Figure 2. Base flow profile of the parameters T_b, ϕ_b, H_b and M_b for (a) $K = +1$ and (b) $K = +1$.

$$\frac{d^2T_b}{dz^2} + \left\{ \frac{N_B}{Le}\frac{d\psi_b}{dz} + \frac{N_A N_B}{Le}\frac{dT_b}{dz} - \frac{N'_A N_B}{Le}\frac{dH_b}{dz} \right\} \frac{dT_b}{dz} + YRC_b = 0, \tag{21}$$

$$\frac{d^2C_b}{dz^2}=0, \tag{22}$$

$$\chi_2\frac{dM_b}{dz}+\frac{dH_b}{dz}=0, \tag{23}$$

$$M_b=\frac{1+\chi}{\chi_2}\left\{\frac{\chi}{1+\chi}H_b-\frac{M_1}{M_2}T_b+\frac{M_1'}{M_2'}\psi_b+\frac{\chi_2-\chi}{1+\chi}\right\}. \tag{24}$$

These Eqs. (19) to (24) are now solved subject to the boundary conditions (17). Thus, we obtained the basis state solution in the form:

$$\begin{aligned}&T_b=A(z)+\frac{T_L}{|T_L-T_U|}R,\ \psi_b=\psi_0-\frac{S_1}{S_2}A(z),\ C_b=1-z,\\&H_b=1+\left(\frac{M_1}{M_2}+\frac{S_1}{S_2}\frac{M_1'}{M_2'}\right)A(z),\ M_b=1-\frac{1}{\chi_2}\left(\frac{M_1}{M_2}+\frac{S_1}{S_2}\frac{M_1'}{M_2'}\right)A(z),\end{aligned} \tag{25}$$

$$\text{where}\quad S_1=N_A-N_A'\frac{M_1}{M_2},\quad S_2=1+N_A'\frac{M_1'}{M_2'},$$

$$\text{and}\quad A(z)=\left(\frac{z^3}{6}-\frac{z^2}{2}\right)RY+\left(\frac{Y}{3}-K\right)Rz.$$

Based on the solution obtained in Eq. (25), the flow profiles (basic state) of T_b,ψ_b,H_b and M_b are presented in Figure 2. Here, the figures are drawn for two different cases, viz., when the system is heated from below (i.e. $K=+1$) and heated from above (i.e. $K=-1$). It is clear from the figures that the base flow profiles of the parameters T_b,ψ_b,H_b and M_b drawn for $K=+1$ is completely different in qualitatively and quantitatively from the base flow profiles drawn for $K=-1$.

PERTURBATION SOLUTION

In this part, firstly, we perturbed the basic state solution as:

$$[\mathbf{v},\ p,\psi,T,C,H,M]=[\mathbf{v}',\ p_b+p',\psi_b+\psi',T_b+\theta',\ C_b+C',H_b+H',M_b+\ M'], \tag{26}$$

where $\mathbf{v}',\ p',\psi',\theta',C',H'$ and M' represent the perturb variables which are assumed to be small.

After utilizing Eq. (26) in Eqs. (11) to (16), linearizing after dropping primes, taking the curl (two times) the z - component of resulting linearized momentum equation together with $H=\nabla\phi,$ the set of Eqs. (11) to (16) takes the form:

$$\begin{aligned}\frac{1}{Pr}\frac{\partial\nabla^2w}{\partial t}=\nabla^4w-\Bigg\{&M_1RA'(z)-R+Ra_N\psi_0-Ra_N\frac{S_1}{S_2}A(z)+R\frac{M_2M_1'}{M_2'}\frac{S_1}{S_2}A'(z)\Bigg\}\nabla_1^2\theta-\Big\{Ra_NA(z)\\&-R\frac{M_2M_1'}{M_2'}A'(z)-Ra_sM_1'\frac{S_1}{S_2}A'(z)+R_n\Bigg\}\nabla_1^2\psi+\left(RM_2+Ra_sM_2'\frac{S_1}{S_2}\right)A'(z)\frac{\partial\nabla_1^2\phi}{\partial z},\end{aligned} \tag{27}$$

$$\frac{\partial\psi}{\partial t}=A'(z)\frac{S_1}{S_2}w+\frac{1}{Le}\nabla^2\psi+\frac{N_A}{Le}\nabla^2\theta-\frac{N_A'}{Le}\frac{\partial}{\partial z}\nabla^2\phi, \tag{28}$$

$$\begin{aligned}\frac{\partial\theta}{\partial t}=-A'(z)w+\nabla^2\theta-\Bigg\{&\frac{N_B}{Le}\frac{S_1}{S_2}A'(z)-\frac{2N_AN_B}{Le}A'(z)+\frac{N_BN_A'M_1}{LeM_2}A'(z)\\&+\frac{N_BN_A'M_1'}{LeM_2'}\frac{S_1}{S_2}A'(z)\Bigg\}\frac{\partial\theta}{\partial z}+\frac{N_B}{Le}\frac{\partial\psi}{\partial z}A'(z)-\frac{N_BN_A'}{Le}A'(z)\frac{\partial^2\phi}{\partial z^2},\end{aligned} \tag{29}$$

$$\frac{\partial C}{\partial t} = w + \eta \nabla^2 C, \tag{30}$$

$$\frac{\partial^2 \phi}{\partial z^2} = \frac{M_1}{M_2}\frac{\partial \theta}{\partial z} - \frac{M_1'}{M_2'}\frac{\partial \psi}{\partial z} - \frac{1+\chi_2}{1+\chi}\nabla_1^2 \phi. \tag{31}$$

Now, a transformation (coordinate) from z to $2z-1$ is applied to adjust the current domain from $[0, 1]$ to $[-1, 1]$. This is so because, to employ the Chebyshev pseudospectral method, the domain must be $[-1, 1]$. Furthermore, the normal mode expansion is considered as:

$$\{w, \theta, \psi, \phi, C\} = \{w(z), \theta(z), \psi(z), \phi(z), C(z)\} \times \exp\{\tau t + i(k_x x + k_y y)\}, \tag{32}$$

where k_x and k_y stands for the wave numbers in x and y direction respectively.

After using the above Eq. (32), the set of Eqs. (27) to (31) takes the following form

$$\begin{aligned}\frac{\tau}{Pr}(4D^2 - k^2)w(z) = (4D^2 - k^2)^2 w(z) + \left\{ M_1 R A'(z_1) - R + Ra_N \phi_0 - Ra_N \frac{S_1}{S_2} A(z_1) \right. \\ \left. + R\frac{M_2 M_1'}{M_2'}\frac{S_1}{S_2}A'(z_1)\right\} k^2 \theta(z) + \left\{ Ra_N A(z_1) - R\frac{M_2 M_1'}{M_2'}A'(z_1) \right. \\ \left. - Ra_s M_1' \frac{S_1}{S_2} A'(z_1) + R_n \right\} k^2 \psi(z) - \left(RM_2 + Ra_s M_2' \frac{S_1}{S_2} \right) 2A'(z_1) k^2 D\phi(z),\end{aligned} \tag{33}$$

$$\tau \psi(z) = A'(z_1)\frac{S_1}{S_2} w + \frac{1}{Le}(4D^2 - k^2)\psi + \frac{N_A}{Le}(4D^2 - k^2)\theta - 2\frac{N_A'}{Le} D(4D^2 - k^2)\phi, \tag{34}$$

$$\begin{aligned}\tau\theta(z) = -A'(z_1)w + (4D^2 - k^2)\theta(z) - 2\left\{ \frac{N_B}{Le}\frac{S_1}{S_2}A'(z_1) - \frac{2N_A N_B}{Le}A'(z_1) + \frac{N_B N_A' M_1}{LeM_2} \right. \\ \left. \times A'(z_1) + \frac{N_B N_A' M_1'}{LeM_2'}\frac{S_1}{S_2}A'(z_1) \right\} D\theta + 2\frac{N_B}{Le}A'(z_1)D\psi - 4\frac{N_B N_A'}{Le}A'(z_1)D^2\phi,\end{aligned} \tag{35}$$

$$\tau C(z) = w + \eta(4D^2 - k^2)C(z), \tag{36}$$

$$4D^2\phi = 2\frac{M_1}{M_2}D\theta - 2\frac{M_1'}{M_2'}D\psi + \left(\frac{1+\chi_2}{1+\chi}\right)k^2\phi. \tag{37}$$

The above set of Eqs. (33) to (37) is to be solved with the following boundary conditions:

$$\left.\begin{aligned} w = \theta = D\psi + N_A D\theta - 2N_A' D^2\phi = C = 0 \quad \text{at} \quad z = \pm 1, \\ 2(1+\chi)D\phi - k\phi = 0 \quad \text{at} \quad z = -1, \\ 2(1+\chi)D\phi + k\phi = 0 \quad \text{at} \quad z = +1, \end{aligned}\right\} \tag{38}$$

with $Dw = 0$ at $z = \pm 1$ for R-R boundaries, $Dw = 0$ at $z = -1$ and $D^2 w = 0$ at $z = +1$ for R-F boundaries, $D^2 w = 0$ at $z = \pm 1$ for F-F boundaries.

NUMERICAL METHOD AND VALIDATION

Equations (33) to (37) subject to the boundary conditions (38) constitute an eigenvalue problem which is now numerically solved by selecting the Chebyshev pseudospectral method.We remark here that the algorithm and procedure mentioned in the paper of Kaloni and Lou [51] are considerately followed in this study. In this procedure, firstly, for a specific value of k, Le, Y, α_L, η and several different physical parameters, we employed the both QZ-algorithm as well as

EIG function in the software MATLAB to evaluate the major eigenvalue (say $\tau = \tau_r + i\tau_i$). Here τ_r and τ_i represent the real and imaginary part of the major eigenvalue respectively. Moreover, the major eigenvalue is considered to be the one which has the largest real part.Thereafter, by employing the Regula Falsi method, we determined that distinctive value of the parameter β corresponding to which τ_r tends to zero. In this manner, we obtained a unique point in the neutral stability curve.To draw the required neutral curve, we repeat the above mentioned process for several other values of k. From the neutral curves, β_c together with k_c can be described as:

$$\beta_c = \min_k \beta(Y, Le, \eta, \mathrm{Pr}.....) \tag{39}$$

where β_c and k_c are the critical temperature gradient and the critical wave number respectively. The Eq. (39) is minimized by utilizing the function FMINBND from MATLAB.

The nature of the stability is also checked numerically by selecting the Chebyshev pseudospectral method. If τ_i i.e. the imaginary part of the major eigenvalue converges to zero simultaneously when τ_r (the real part) converges to zero, then the stability is called non-oscillatory (or stationary).On the contrary, if τ_i does not tends to zero simultaneously when the real part τ_r converges to zero, then the stability is known as oscillatory.To examine the nature of stability, the leading eigenvalue $\tau = \tau_r + i\tau_i$ is determined for all the non-dimensional parameters and it is noticed that τ_i always tends to zero at the same time when τ_r tends to zero.In this way, it is observed that the stability for the considered problem is stationary for both the two considered configurations.

Table 1. Value of k_c^2 and Ra_c.

		Hill[2]		Presentwork	
K	Y	k_c^2	Ra_c	k_c^2	Ra_c
+1	1	5.882	252.268	5.848	252.268
	10	5.545	28.698	5.516	28.698
-1	1	5.064	343.235	5.050	343.234
	10	5.459	29.591	5.435	29.591

To figure out the accuracy of the numerical method applied in the present work, we solved our problem in the nonappearance of the external magnetic field and nanoparticles for R--R boundaries using our code. The results are determined for $\eta = 0.01$. From Table 1, it is clear that the results derived in the present study are in best agreement with the previously published results of Hill [2].

RESULTS AND DISCUSSION

We employed the linear stability theory and derived the results for R-R, R-F and F-F boundaries. The obtained results are presented graphically in Figs. 3-7 and also in tabular form in Table II for the two different cases, viz., when the system is heated from below (i.e. $K = +1$) and heated from above (i.e. $K = -1$).

The values of the physical quantities utilized in the present work are considered as follows: density $\rho_f = 1180$, thermal conductivity $\mathrm{k}_1 = 0.59$, magnetic saturation $\mathrm{M}_s = 15,900$, viscosity $\mu = 0.007$, thermal expansion coefficient $\alpha = 5.2e-4$, Prandtl number Pr=42.1.

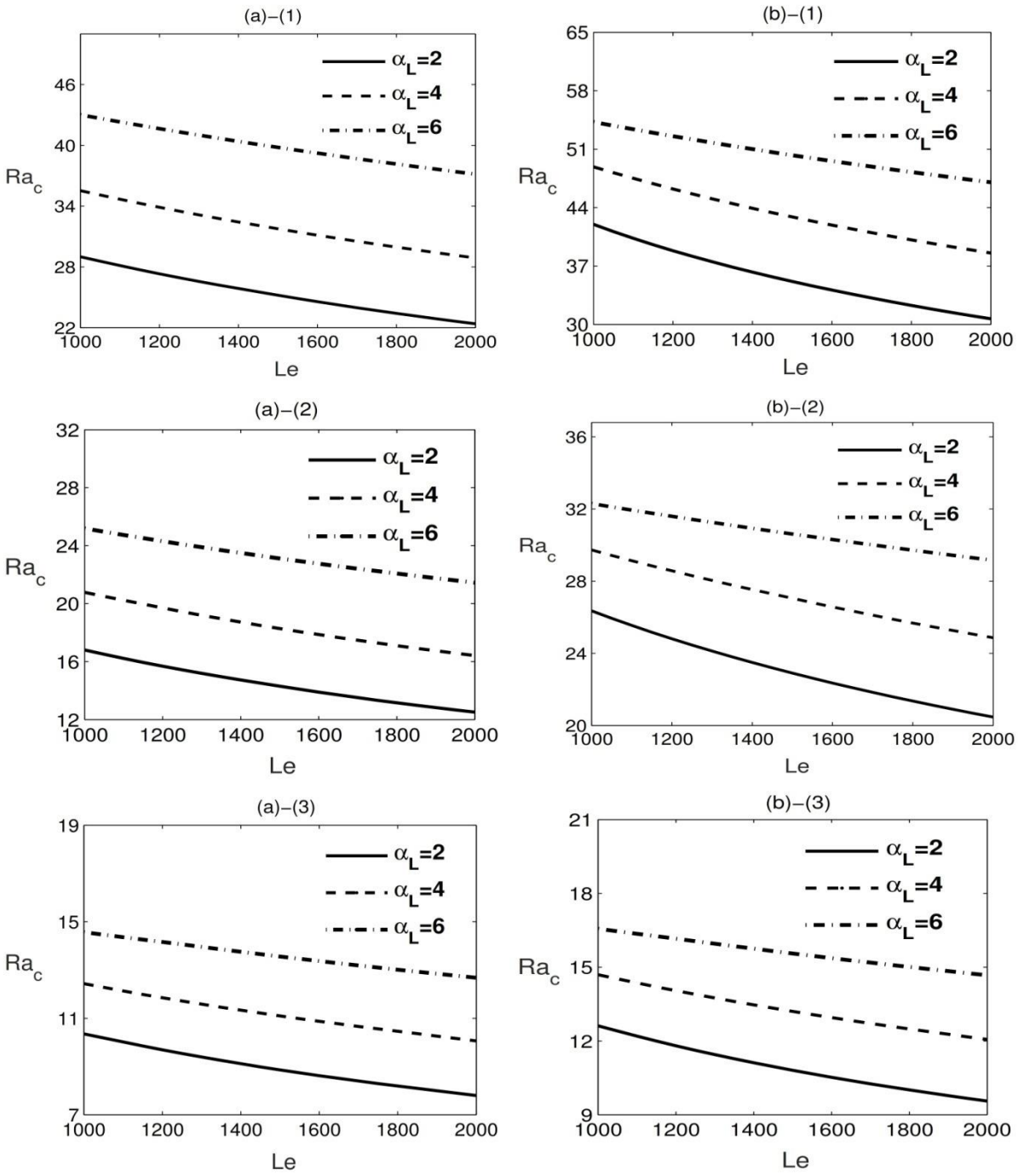

Figure 3. Locus of Ra_c and Le for three various values of the parameter α_L for (a) $K = +1$ and (b) $K = -1$ for (1) R-R, (2) R-F and (3) F-F boundaries.

The effect of both MNF Lewis number Le and Langevin parameter α_L on Ra_c (the critical Rayleigh number) is presented simultaneously in Figure 3 for two different cases, viz., when the layer is heated from below and heated from above. From the figure, it is seen that the value of the parameter Ra_c increases as α_L increases. This is due to the fact that the existence of an internal heat source gives rise to the forces that dominate the magnetic forces. As the value of α_L increase, the influence of the magnetic field also increases in the system, which in turn decelerates the disturbance in the MNF layer. It is also evident from Figure 3 that with an increase in the value of the Lewis number Le, value of the parameter Ra_c decreases. Thus, α_L has a stabilizing impact on the system; on the contrary, the Lewis number Le has a destabilizing impact on the considered system. These results are in agreement with those observed by Kaloni and Lou [50] and Nield and Kuznetsov [15].

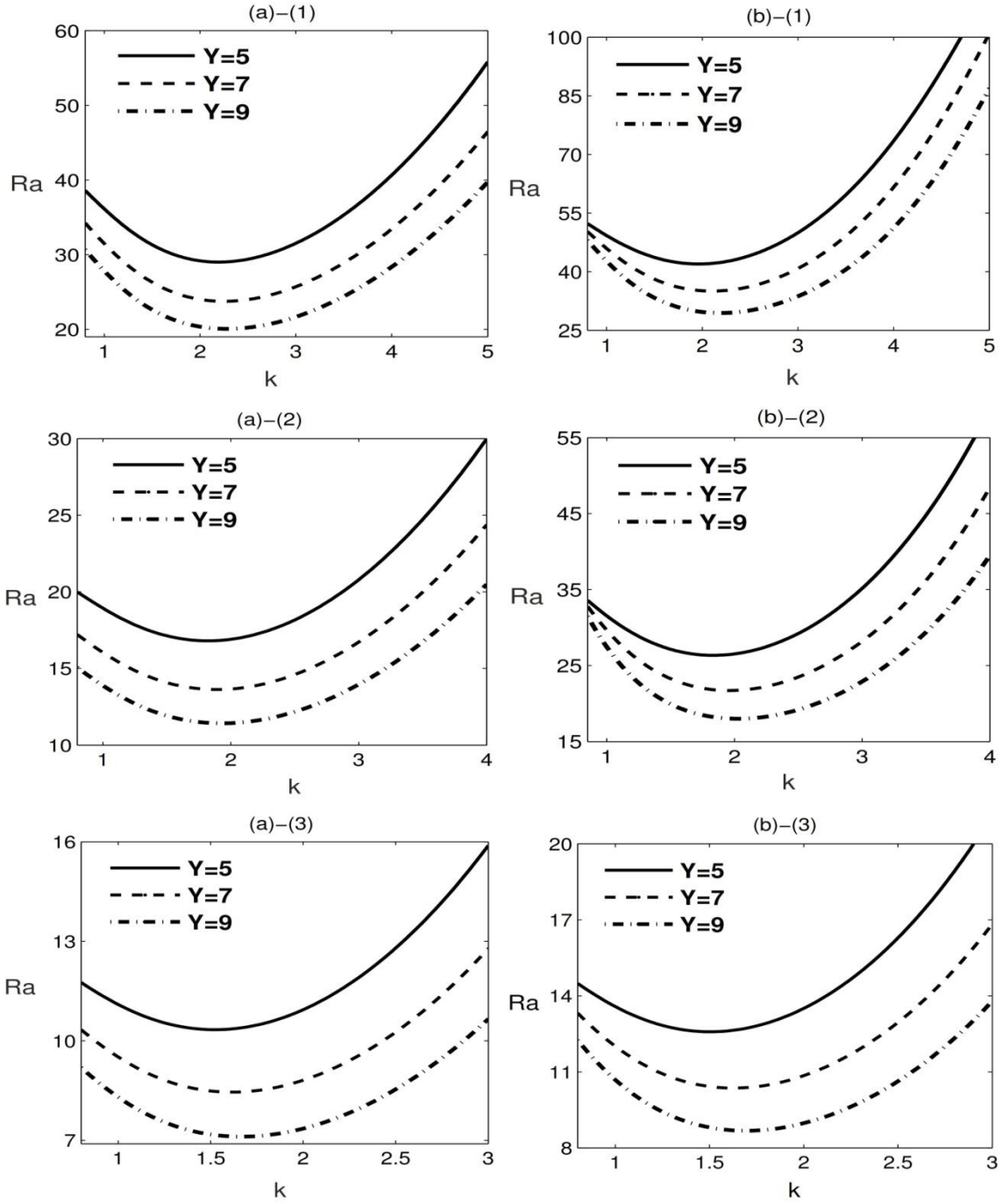

Figure 4. Neutral curves for various values of the parameter Y for (a) $K = +1$ and (b) $K = -1$ for (1) R-R, (2) R-F and (3) F-F boundaries

To examine the impact of the selective absorption of radiation on the stability of the system, the neutral curves for three different value of the parameter Y are illustrated in Figure 4. It can be seen from the figure that with an increase in the value of the parameter Y, the value of the parameter Ra_c decrease. The parameter Y is the ratio of internal heating to boundary heating, and therefore as the value of the parameter Y increases, the strength of the radiative heating increases, which in turn decreases the general stability of the system. In this way, the parameter Y hasten the onset of MNF convection.

.

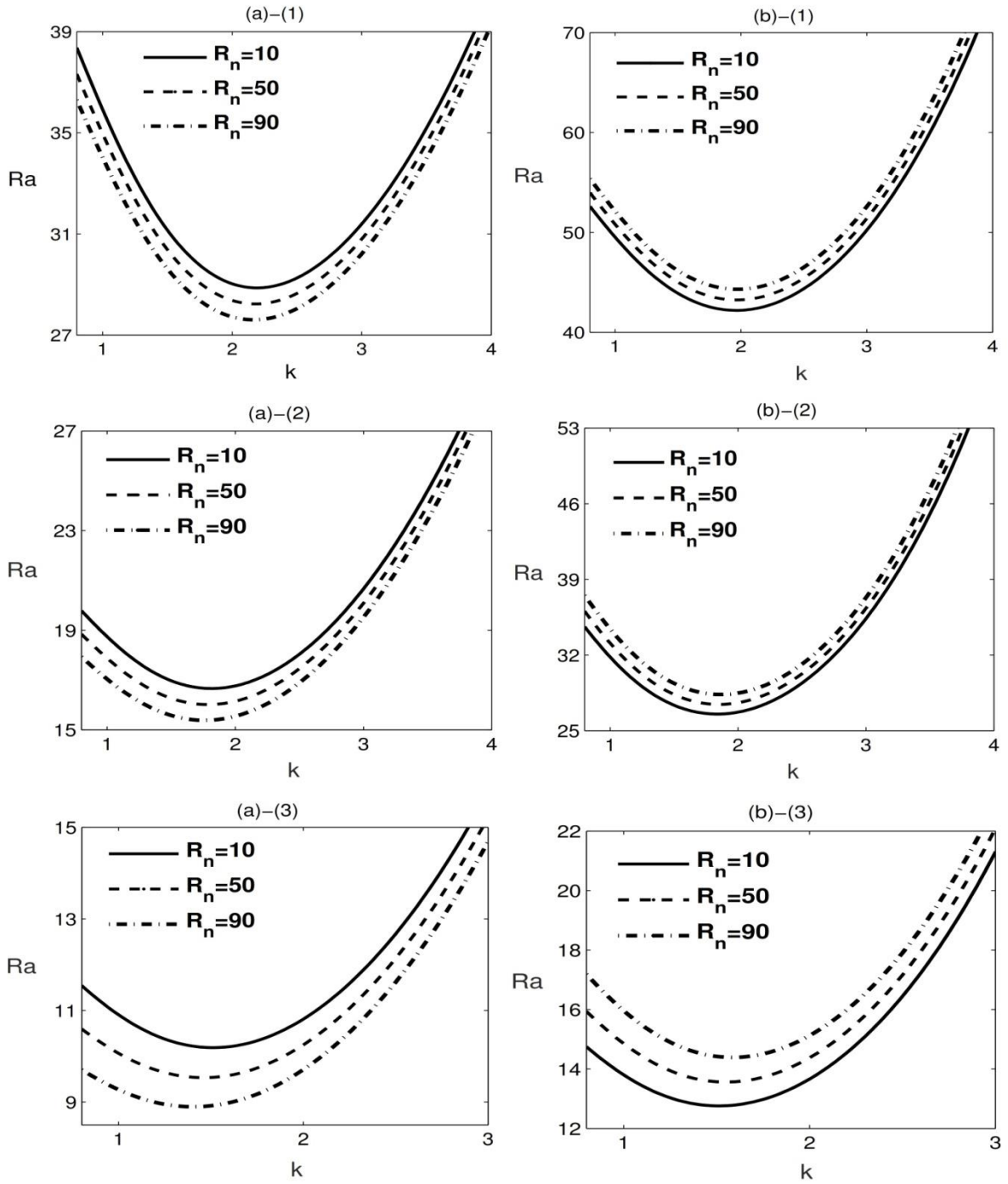

Figure 5. Neutral curves for three various values of the parameter R_n for (a) $K = +1$ and (b) $K = -1$; for (1) R-R, (2) R-F and (3) F-F boundaries

Figure 5 represents the neutral stability curve for different value of R_n. It is clear from the graphs that for $K = +1$, the curves move downward with an increment in the value of the parameter R_n and thus the value of Ra_c decreases. However, for the case when $K = -1$, the value of the parameter Ra_c increases as R_n increases. In this way, the parameter R_n expedites the convection process for $K = +1$ and decelerates the onset of convection for $K = -1$. The reason for such a qualitative change in the behavior of R_n is the pattern of magnetic nanoparticle distribution (that is, whether it is top-heavy or bottom-heavy). It can be seen from Figure 2 that the magnetic nanoparticle distribution is top-heavy for $K = +1$ and bottom-heavy when $K = -1$. Earlier Nield and Kuznetsov [12] observed a destabilizing behavior of R_n for the top-heavy nanoparticle distribution, whereas, a stabilizing impact of the parameter R_n was reported in several studies including [27, 53].

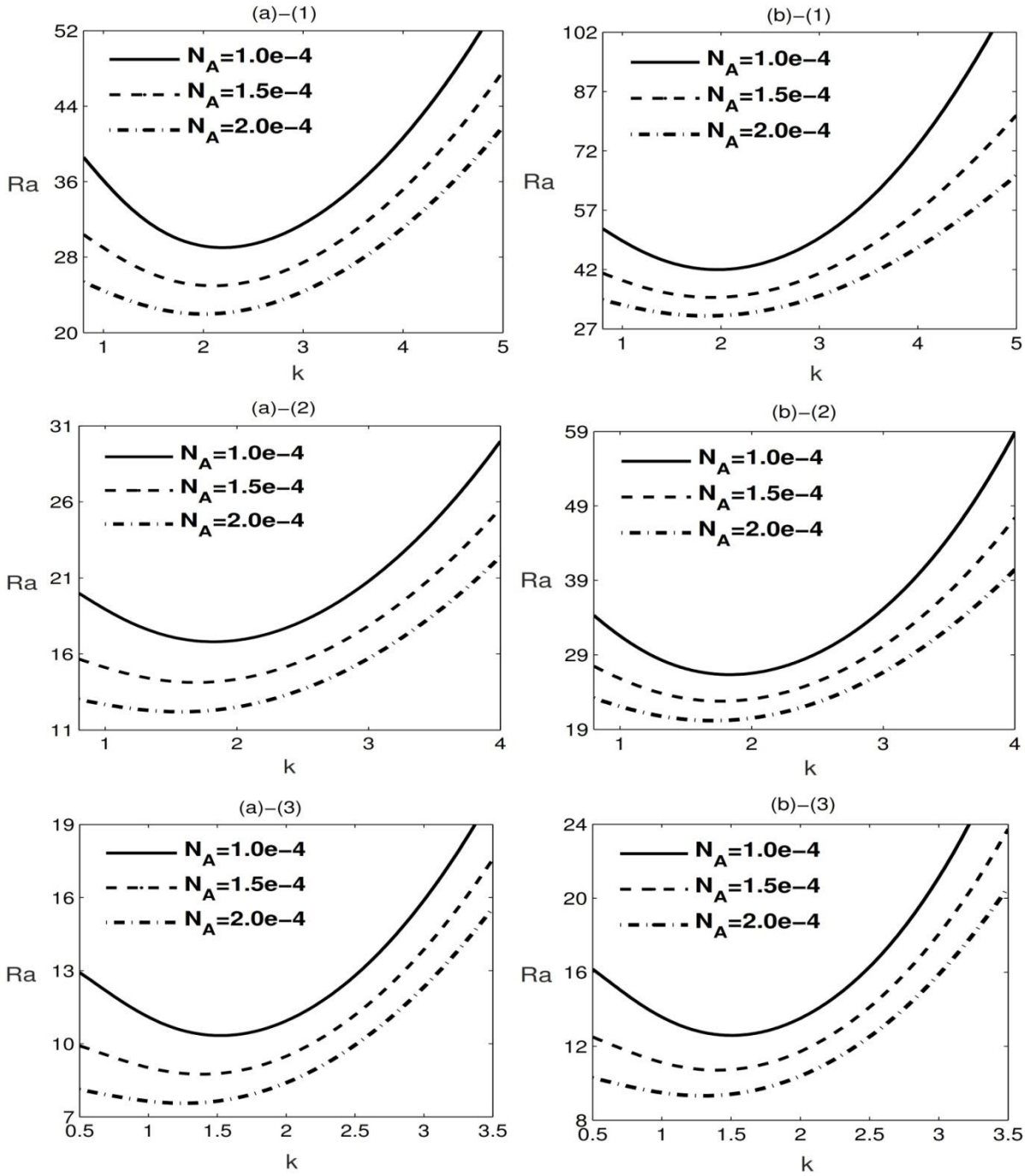

Figure 6. Neutral curves for three various values of the parameter N_A for (a) $K = +1$ and (b) $K = -1$ for (1) R-R, (2) R-F and (3) F-F boundaries

The effect of the parameter N_A on the variation of the neutral stability curve is depicted in Figure 6. The impact of increasing the value of N_A is seen to expedites the onset of MNF convection. This is so because, thermophoretic diffusion, which is one of the principal forces related to the motion of magnetic nanoparticles promoted as the value of the parameter N_A increases. For a larger value of thermophoretic diffusivity, thermophoresis generates a kind of unrest in MNF layer, which in turn allowing convection to commence more easily. Thus the value of the parameter Ra_c decreases with an increase in the value of the parameter N_A.

Figure 7 presents the variation of Ra with k for several values of the diffusivity ratio η. It is clearly seen from the figure that with an increase in the value of the parameter η, the value of Ra_c increases. Such behavior of the parameter η remains the same for both the two configurations (that is for $K = +1$ and $K = -1$). A larger value of η slows down the thermophoretic diffusion which in turn leads to a larger value of Ra_c. In this way, the parameter η slows down the

onset of convection. An identical behavior was earlier noticed by Straughan [3] in the nonappearance of both the magnetic field as well as nanoparticles concentration.

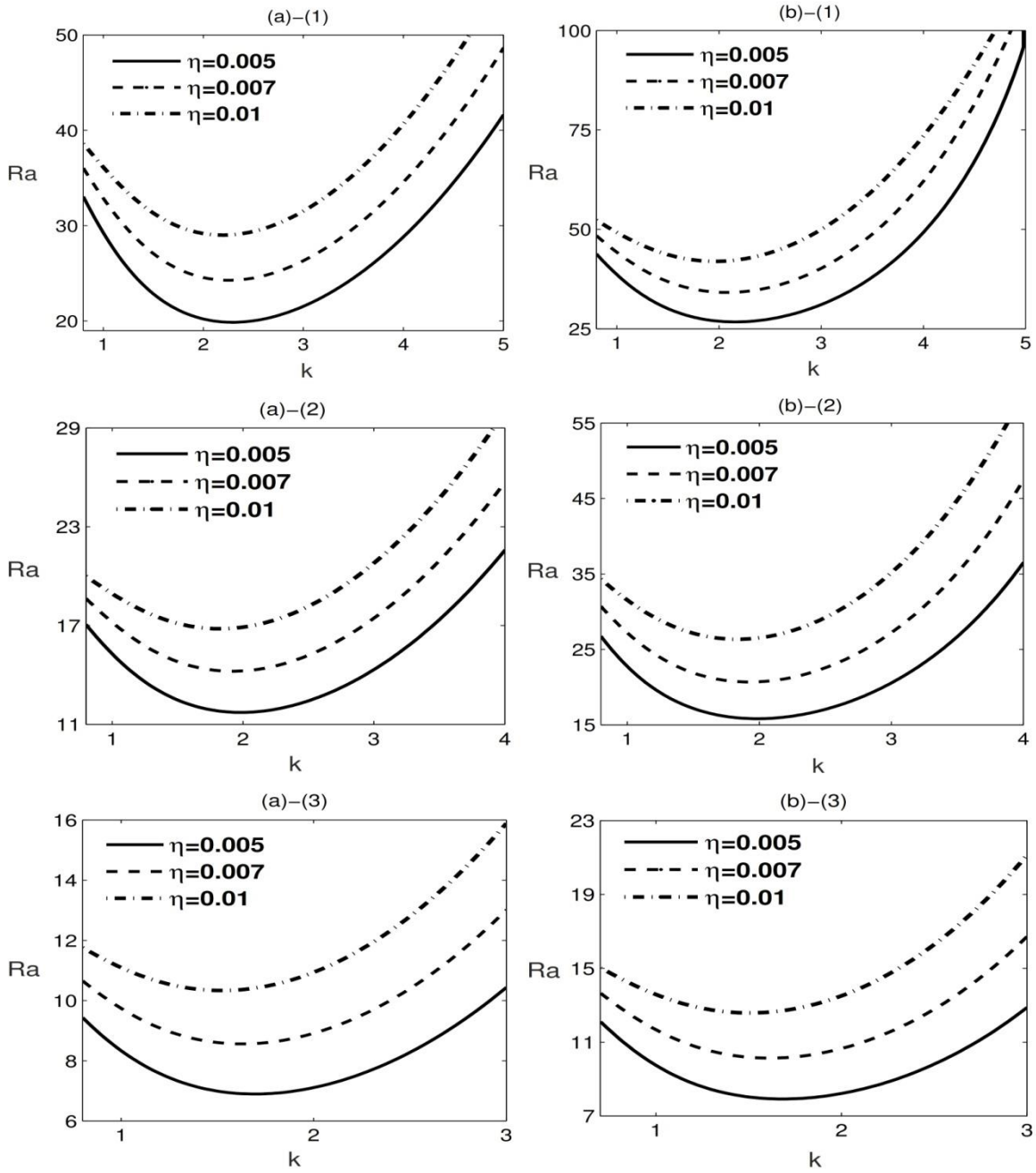

Figure 7. Neutral curves for three various values of the parameter η for (a) $K=+1$ and (b) $K=-1$; for (1) R-R, (2) R-F and (3) F-F boundaries

The neutral stability curves for different values of the nanoparticle volume fraction ψ_0 are shown in Figure 8. For the case when $K=+1$, the figures show that the critical value of the parameter Ra decreases when the value of ψ_0 increasing. However, for $K=-1$, it is noticed that the value of Ra_c increases as the value of ψ_0 increases. Thus the behavior of ψ_0 is different for both the cases i.e. when $K=+1$ and when $K=-1$. The reason behind such variation in the behavior of ψ_0 is the change in its base flow profile of ψ_b. It can be seen from Figure 2 that the magnetic nanoparticle distribution is top-heavy for $K=+1$ and bottom-heavy when $K=-1$. Thus ψ_0 destabilize the system when $K=+1$, and stabilize the system when $K=-1$.

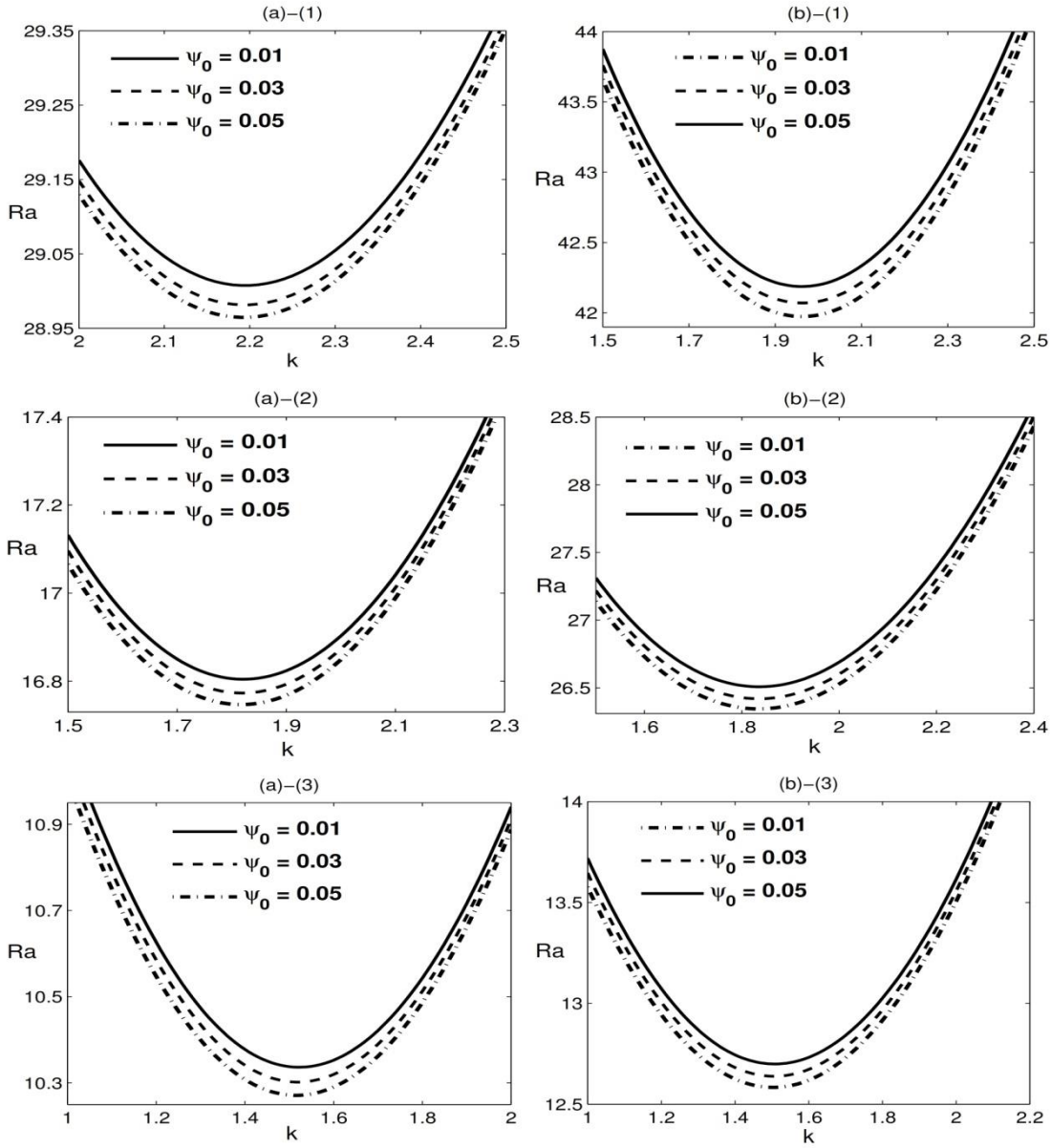

Figure 8. Neutral curves for various values of the parameter ψ_0 for (a) $K = +1$ and (b) $K = -1$; for (1) R-R, (2) R-F and (3) F-F boundaries

Table 2 illustrates the values of the parameters k_c and Ra_c for several values of η and Y for water-based MNF. The primary reason for presenting this table is to investigate the impact of one significant parameter (i.e. selective absorption of radiation) on the onset of convection. For this purpose, the effect of several values of Y on k_c and Ra_c is shown in Table 2 for R-R, R-F, and F-F boundaries. These values are calculated for both $K = +1$ as well as for $K = -1$ for R-R, R-F, and F-F boundary conditions. It is clearly seen from the table 2 that for a specific value of η, as the value of the parameter Y increases, the value of Ra_c decreases for both the cases $K = +1$ and $K = -1$. Thus the parameter Y always hasten the onset of convection. Earlier, Hill [2] and Straughan [3] made a similar observation for the parameter Y in the case when the magnetic field and nanoparticle concentration are not presented in the system. It can also be seen from the table that with an increase in the value of η, the value of Ra_c always increases for both the two configurations (that is, $K = +1$ and $K = -1$). Thus the parameter η always delays the onset of MNF convection.

Table 2. Effect of $K, \eta,$ and Y on k_c and Ra_c.

			R-R		R-F		F-F	
K	η	Y	k_c	Ra_c	k_c	Ra_c	k_c	Ra_c
+1	0.001	1	2.30	20.77	2.02	12.67	1.71	7.11
		3	2.34	8.65	2.08	5.15	1.79	2.83
		5	2.35	5.44	2.09	3.21	1.80	1.75
		7	2.34	3.96	2.10	2.33	1.81	1.26
		10	2.34	2.81	2.10	1.65	1.81	0.89
	0.01	1	1.55	49.64	1.00	28.90	1.00	16.21
		3	2.07	37.01	1.66	21.67	1.31	13.01
		5	2.19	29.01	1.82	16.80	1.52	10.34
		7	2.25	23.75	1.89	13.63	1.61	8.46
		10	2.29	18.61	1.94	10.56	1.68	6.58
-1	0.001	1	2.13	26.07	1.93	14.94	1.66	7.78
		3	2.28	9.82	2.06	5.67	1.78	2.97
		5	2.31	5.93	2.08	3.44	1.80	1.81
		7	2.32	4.23	2.09	2.46	1.80	1.30
		10	2.33	2.95	2.10	1.72	1.81	0.91
	0.01	1	1.00	55.15	1.00	33.57	1.00	17.49
		3	1.70	49.65	1.56	31.26	1.22	15.26
		5	1.96	41.97	1.83	26.35	1.50	12.58
		7	2.10	35.04	1.96	21.71	1.63	10.36
		10	2.22	27.10	2.05	16.47	1.71	8.00

CONCLUSIONS

In this paper, the study of MNF convection stimulated by selective absorption of radiation is conducted by employing the linear stability analysis. An appropriate non-dimensional scaling is employed to derive a dimensionless set of governing equations. The obtained eigenvalue problem is solved by selecting the Chebyshev pseudospectral method for the R-R, R-F and F-F boundary conditions. The results are derived for two different types of configurations, viz., when the system is heated from the below and when the system is heated from the above. It is also assumed that the flux of nanoparticle remains zero at both the lower and upper boundaries. The results show that the effect of an increase in the value of the parameters α_L and η is to increase the value of Ra_c, and hence decelerate the onset of convection for all the three types of boundary conditions. On the contrary, an increment in the value of the parameters Le, Y, N_A speed up the onset of MNF convection. In addition, the parameter R_n expedite the onset of MNF convection in the case when the fluid layer is heated from the below, whereas decelerates the onset of MNF in the case when the fluid layer is heated from the above. The principle of exchange of stability is also found to be valid for the present problem.

ACKNOWLEDGMENTS

The authors would like to acknowledged CSIR (Council of Scientific and Industrial Research), New Delhi for the financial support in the form of R & D (Research and Development) project [number 25(0255)/16/EMR-II].

REFERENCES

[1] R. Krishnamurti, "Convection induced by selective absorption of radiation: A laboratory model of conditional instability," *Dyn. of Atm. And Ocean,* vol. 27, no. 1-4, pp. 367-382, 1998, doi: 10.1016/s0377-0265(97)00020-1.

[2] A. A. Hill, "Penetrative convection induced by the absorption of radiation with a nonlinear internal heat source," *Dyn. of Atm. And Ocean,* vol. 38, no. 1, pp. 57-67, 2004, doi: 10.1016/j.dynatmoce.2004.03.002.

[3] B. Straughan, "Global stability for convection induced by absorption of radiation," *Dyn. of Atm. And Ocean,* vol. 35, no. 4, pp. 351-361, 2002, doi: 10.1016/S0377-0265(02)00051-9.

[4] A. A. Hill, "Convection due to the selective absorption of radiation in a porous medium," *Continuum Mech. Thermodyn.,* vol. 15, no. 5, pp. 451-462, 2003, doi: 10.1007/s00161-003-0125-5.

[5] M. H. Chang, "Stability of convection induced by selective absorption of radiation in a fluid overlying a porous layer," *Phys. Fluids,* vol. 16, no. 10, pp. 3690-3698, 2004, doi: 10.1063/1.1789551.

[6] A. A. Hill, "Convection induced by the selective absorption of radiation for the Brinkman model," *Continuum Mech. Thermodyn.,* vol. 16, no. 1-2, pp. 43-52, 2004, doi: 10.1007/s00161-003-0140-6.

[7] A. J. Harfash, "Three dimensional simulations and stability analysis for convection induced by absorption of radiation," *Int. J. Numer. Methods Heat Fluid Flow,* vol. 25, no. 4, pp. 810-824, 2015, doi: 10.1108/HFF-08-2013-0250.

[8] J. Buongiorno, "Convective transport in nanofluids," *J. Heat Transfer,* vol. 128, no. 3, pp. 240-250, 2006, doi: 10.1115/1.2150834.

[9] D. Y. Tzou, "Instability of nanofluids in natural convection," *J. Heat Transfer,* vol. 130, no. 7, 2008, doi: 10.1115/1.2908427.

[10] D. A. Nield, and A. V. Kuznetsov, "The onset of convection in a horizontal nanofluid layer of finite depth," *Eur. J. Mech. B. Fluids,* vol. 29, no. 3, pp. 217-223, 2010, doi: 10.1016/j.euromechflu.2010.02.003.

[11] D. A. Nield, and A. V. Kuznetsov, "The onset of convection in a horizontal nanofluid layer of finite depth: A revised model," *Int. J. Heat Mass Transfer,* vol. 77, pp. 915-918, 2014, doi: 10.1016/j.ijheatmasstransfer.2014.06.020.

[12] D. A. Nield, and A. V. Kuznetsov, "Thermal instability in a porous medium layer saturated by a nanofluid," *Int. J. Heat Mass Transfer,* vol. 52, no. 25-26, pp. 5796-5801, 2009, doi: 10.1016/j.ijheatmasstransfer.2009.07.023.

[13] D. Yadav, G. S. Agrawal, and R. Bhargava, "Thermal instability of rotating nanofluid layer," *Int. J. Eng. Sci.,* vol. 49, no. 11, pp. 1171-1184, 2011, doi: 10.1016/j.ijengsci.2011.07.002.

[14] D. Yadav, R. Bhargava, and G. S. Agrawal, "Boundary and internal heat source effects on the onset of Darcy-Brinkman convection in a porous layer saturated by nanofluid," *Int. J. Therm. Sci.,* vol. 60, pp. 244-254, 2012, doi: 10.1016/j.ijthermalsci.2012.05.011.

[15] D. A. Nield, and A. V. Kuznetsov, "The onset of convection in an internally heated nanofluid layer," *J. Heat Transfer,* vol. 136, no. 1, 2014, doi: 10.1115/1.4025048.

[16] K. Zaimi, A. Ishak, and I. Pop, "Boundary layer flow and heat transfer over a nonlinearly permeable stretching/shrinking sheet in a nanofluid," *Sci. Rep.,* vol. 4, no. 1, pp. 1-8, 2014, doi: 10.1038/srep04404.

[17] R. A. Hamid, R. Nazar, and I. Pop, "Non-alignment stagnation-point flow of a nanofluid past a permeable stretching/shrinking sheet: Buongiorno's model," *Sci. Rep.,* vol. 5, no. 1, pp. 14640-14640, 2015, doi: 10.1038/srep14640.

[18] A. I. Alsabery, M. A. Sheremet, A. J. Chamkha, and I. Hashim, "MHD convective heat transfer in a discretely heated square cavity with conductive inner block using two-phase nanofluid model," *Sci. Rep.,* vol. 8, no. 1, pp. 1-23, 2018, doi: 10.1038/s41598-018-25749-2.

[19] M. Sheikholeslami, I. Khan, and I. Tlili, "Non-equilibrium Model for Nanofluid Free Convection Inside a Porous Cavity Considering Lorentz Forces," *Sci. Rep.,* vol. 8, no. 1, pp. 1-13, 2018, doi: 10.1038/s41598-018-33079-6.

[20] D. Yadav, "The onset of longitudinal convective rolls in a porous medium saturated by a nanofluid with non-uniform internal heating and chemical reaction," *J. Therm. Anal. Calorim.,* vol. 135, no. 2, pp. 1107-1117, 2019, doi: 10.1007/s10973-018-7748-z.

[21] G. C. Rana, H. Saxena, and P. K. Gautam, "The Onset of Electrohydrodynamic Instability in a Couple-Stress Nano-fluid Saturating a Porous Medium: Brinkman Mode | Revista Cubana de Física," *Rev. Cubana Fis.,* vol. 36, no. 1, pp. 37-45, 2019.

[22] D. Yadav, and J. Wang, "Convective Heat Transport in a Heat Generating Porous Layer Saturated by a Non-Newtonian Nanofluid," *Heat Transfer Eng.,* vol. 40, no. 16, pp. 1363-1382, 2019, doi: 10.1080/01457632.2018.1470298.

[23] A. Alhashash, "Natural convection of Nanoliquid from a Cylinder in Square Porous Enclosure using Buongiorno's Two-phase Model," *Sci. Rep.,* vol. 10, no. 1, pp. 1-12, 2020, doi: 10.1038/s41598-019-57062-x.

[24] D. Yadav, "Numerical solution of the onset of Buoyancy ‐ driven nanofluid convective motion in an anisotropic porous medium layer with variable gravity and internal heating," *Heat Transfer,* vol. 49, no. 3, pp. 1170-1191, 2020.

[25] O. Mahian, L. Kolsi, M. Amani, P. Estellé, G. Ahmadi, C. Kleinstreuer, J. S. Marshall, M. Siavashi, R. A. Taylor, H. Niazmand, S. Wongwises, T. Hayat, A. Kolanjiyil, A. Kasaeian, and I. Pop, "Recent advances in modeling and simulation of nanofluid flows-Part I: Fundamentals and theory," Elsevier B.V., 2019, pp. 1-48.

[26] O. Mahian, L. Kolsi, M. Amani, P. Estellé, G. Ahmadi, C. Kleinstreuer, J. S. Marshall, R. A. Taylor, E. Abu-Nada, S. Rashidi, H. Niazmand, S. Wongwises, T. Hayat, A. Kasaeian, and I. Pop, "Recent advances in modeling and simulation of nanofluid flows—Part II: Applications," Elsevier B.V., 2019, pp. 1-59.

[27] U. Gupta, J. Ahuja, and R. K. Wanchoo, "Magneto convection in a nanofluid layer," *Int. J. Heat Mass Transfer,* vol. 64, pp. 1163-1171, 2013, doi: 10.1016/j.ijheatmasstransfer.2013.05.035.

[28] D. Yadav, R. Bhargava, and G. S. Agrawal, "Thermal instability in a nanofluid layer with a vertical magnetic field," *J. Eng. Math.,* vol. 80, pp. 147-164, 2013, doi: 10.1007/s10665-012-9598-1.

[29] D. Yadav, "The effect of pulsating throughflow on the onset of magneto convection in a layer of nanofluid confined within a Hele-Shaw cell," *Proc. Inst. Mech. Eng., Part E,* vol. 233, no. 5, pp. 1074-1085, 2019, doi: 10.1177/0954408919836362.

[30] L. Kolsi, A. Abidi, M. N. Borjini, and H. B. Aïssia, "The effect of an external magnetic field on the entropy generation in three-dimensional natural convection," *Therm. Sci.,* vol. 14, no. 2, pp. 341-352, 2010, doi: 10.2298/TSCI1002341K.

[31] C. Maatki, L. Kolsi, H. F. Oztop, A. Chamkha, M. N. Borjini, H. B. Aissia, and K. Al-Salem, "Effects of magnetic field on 3D double diffusive convection in a cubic cavity filled with a binary mixture," *Int. Commun. Heat Mass Transfer,* vol. 49, pp. 86-95, 2013, doi: 10.1016/j.icheatmasstransfer.2013.08.019.

[32] M. A. Ismael, M. A. Mansour, A. J. Chamkha, and A. M. Rashad, "Mixed convection in a nanofluid filled-cavity with partial slip subjected to constant heat flux and inclined magnetic field," *J. Magn. Magn. Mater.,* vol. 416, pp. 25-36, 2016, doi: 10.1016/j.jmmm.2016.05.006.

[33] M. M. Rashidi, M. Nasiri, M. Khezerloo, and N. Laraqi, "Numerical investigation of magnetic field effect on mixed convection heat transfer of nanofluid in a channel with sinusoidal walls," *J. Magn. Magn. Mater.,* vol. 401, pp. 159-168, 2016, doi: 10.1016/j.jmmm.2015.10.034.

[34] D. Yadav, R. Bhargava, G. S. Agrawal, G. S. Hwang, J. Lee, and M. C. Kim, "Magneto-convection in a rotating layer of nanofluid," *Asia-Pac. J. Chem. Eng.,* vol. 9, no. 5, pp. 663-677, 2014, doi: 10.1002/apj.1796.

[35] D. Yadav, C. Kim, J. Lee, and H. H. Cho, "Influence of magnetic field on the onset of nanofluid convection induced by purely internal heating," *Comput. Fluids,* vol. 121, pp. 26-36, 2015, doi: 10.1016/j.compfluid.2015.07.024.

[36] M. Sheikholeslami, "CuO-water nanofluid free convection in a porous cavity considering Darcy law," *Eur. Phys. J. Plus,* vol. 132, no. 1, pp. 1-11, 2017, doi: 10.1140/epjp/i2017-11330-3.

[37] I. Nkurikiyimfura, Y. Wang, and Z. Pan, "Heat transfer enhancement by magnetic nanofluids - A review," Elsevier Ltd, 2013, pp. 548-561.

[38] B. A. Finlayson, "Convective instability of ferromagnetic fluids," *J. Fluid Mech.,* vol. 40, no. 4, pp. 753-767, 1970, doi: 10.1017/S0022112070000423.

[39] A. Mahajan, and M. Arora, "Convection in Magnetic Nanofluids," *J. Nanofluids,* vol. 2, no. 2, pp. 147-156, 2013, doi: 10.1166/jon.2013.1045.

[40] A. Mahajan, and M. K. Sharma, "Convection in magnetic nanofluids in porous media," *J. Porous Media,* vol. 17, no. 5, pp. 439-455, 2014, doi: 10.1615/JPorMedia.v17.i5.60.

[41] M. Sheikholeslami, M. M. Rashidi, T. Hayat, and D. D. Ganji, "Free convection of magnetic nanofluid considering MFD viscosity effect," *J. Mol. Liq.,* vol. 218, pp. 393-399, 2016, doi: 10.1016/j.molliq.2016.02.093.

[42] M. Sheikholeslami, "Numerical simulation of magnetic nanofluid natural convection in porous media," Elsevier B.V., 2017, pp. 494-503.

[43] M. S. Kandelousi, "Effect of spatially variable magnetic field on ferrofluid flow and heat transfer considering constant heat flux boundary condition," *Eur. Phys. J. Plus,* vol. 129, no. 11, pp. 1-12, 2014, doi: 10.1140/epjp/i2014-14248-2.

[44] M. Sheikholeslami, and M. M. Rashidi, "Ferrofluid heat transfer treatment in the presence of variable magnetic field," *Eur. Phys. J. Plus,* vol. 130, no. 6, pp. 1-12, 2015, doi: 10.1140/epjp/i2015-15115-4.

[45] A. Mahajan, and M. K. Sharma, "Penetrative convection in magnetic nanofluids via internal heating," *Phys. Fluids,* vol. 29, no. 3, pp. 034101-034101, 2017, doi: 10.1063/1.4977091.

[46] A. Mahajan, and M. K. Sharma, "The onset of penetrative convection stimulated by internal heating in a magnetic nanofluid saturating a rotating porous medium," *Can. J. Phys.,* vol. 96, no. 8, pp. 898-911, 2018, doi: 10.1139/cjp-2017-0640.

[47] A. Mahajan, and M. K. Sharma, "The onset of convection in a magnetic nanofluid layer with variable gravity effects," *Appl. Math. Comput.,* vol. 339, pp. 622-635, 2018, doi: 10.1016/j.amc.2018.07.062.

[48] A. Mahajan, and M. K. Sharma, "Penetrative convection due to absorption of radiation in a magnetic nanofluid saturated porous layer," *Studia Geotechnica et Mechanica,* vol. 41, no. 3, pp. 129-142, 2019, doi: 10.2478/sgem-2019-0018.

[49] R. E. Rosensweig, *Ferrohydrodynamics*: Courier Corporation, 2013.

[50] P. N. Kaloni, and J. X. Lou, "Convective instability of magnetic fluids," *Phys. Rev. E: Stat. Phys. Plasmas Fluids Relat. Interdiscip. Top,* vol. 70, no. 2, pp. 12-12, 2004, doi: 10.1103/PhysRevE.70.026313.

[51] M. I. Shliomis, and B. L. Smorodin, "Convective instability of magnetized ferrofluids," *J. Magn. Magn. Mater.,* vol. 252, no. 1-3 SPEC. ISS., pp. 197-202, 2002, doi: 10.1016/S0304-8853(02)00712-6.

[52] B. Straughan, *The Energy Method, Stability, and Nonlinear Convection*, New York, NY: Springer New York, 2004.

[53] U. Gupta, J. Sharma, and V. Sharma, "Instability of binary nanofluids with magnetic field," *Appl. Math. Mech.,* vol. 36, no. 6, pp. 693-706, 2015, doi: 10.1007/s10483-015-1941-6.